

Velocity correlations in dense granular flows observed with internal imaging

Ashish V. Ojpe and Arshad Kudrolli

Department of Physics, Clark University, Worcester, Massachusetts 01610

(Dated: March 23, 2024)

Abstract

We show that the velocity correlations in uniform dense granular flows inside a silo are similar to the hydrodynamic response of an elastic hard-sphere liquid. The measurements are made using a fluorescent refractive index matched interstitial fluid in a regime where the flow is dominated by grains in enduring contact and fluctuations scale with the distance traveled, independent of flow rate. The velocity autocorrelation function of the grains in the bulk shows a negative correlation at short time and slow oscillatory decay to zero similar to simple liquids. Weak spatial velocity correlations are observed over several grain diameters. The mean square displacements show an inflection point indicative of caging dynamics. The observed correlations are qualitatively different at the boundaries.

PACS numbers: 45.70.Ht, 45.70.Mg

The structure and dynamics of dense granular flows is a problem of fundamental interest. Investigating the correlations in the fluctuations of the grain motion can yield insight into the caging and diffusion of particles. And as measured by the velocity auto-correlation functions, they can also illustrate memory in the motion of the constituents. Having a measure of the correlations is important in developing a hydrodynamic description for granular materials and interpretation of variables used to characterize their properties.

Considerable relevant work exists in the context of simple fluids modeled as elastic hard spheres [1]. Computer simulations have shown that the velocity autocorrelation function of dense elastic particles in equilibrium exhibit a negative correlation at short times due to backscatter [2]. The resulting coupling of the tagged particle to the hydrodynamic modes are implicated in the observation of power law decays of velocity [3], which is in contrast with the anticipated exponential decay based on Markovian interactions of particles with neighbors. These effects were later described by hydrodynamic and mode-coupling theories [4, 5], and are said to be in excellent agreement with direct observations in colloidal systems [6, 7]. Thus correlations are observed even in simple dense liquids where particles interact elastically.

In granular systems, because inelasticity and friction is important whenever grains come in contact, relative motion is suppressed unless energy is supplied externally. Thus it is unclear if correlations present in granular systems are similar to simple liquids [8]. Recently, fluctuations and correlations have been reported in dense granular systems, but the observations without exception have been made next to the sidewalls or at the free surface [9, 10, 11, 12, 13]. The source for correlations are complicated by the direct influence of the boundary on caging and diffusion, and the presence of shear in the location where the observations are made.

Here, we examine simplified uniform dense granular flows which occur inside a silo away from the side walls to compare and contrast their fluctuation properties with simple liquids in equilibrium. We use a fluorescent refractive index matched liquid technique [14, 15] to measure the correlations in motion of the grains in the bulk, and further compare it with those near the sidewalls. The fluctuation properties of the particles are observed to be independent of the flow rate, and therefore the interstitial fluid has no significant effect on the grain fluctuations in our experiments. We find that the correlations in the granular fluctuations as measured by the mean square displacements, and the velocity auto-correlation function are remarkably similar to that observed in elastic hard sphere liquids. Thus our

measurements support hydrodynamic approaches for granular systems using approximations made for many-body correlations as for simple liquids.

The experimental apparatus consists of a glass silo chamber with dimensions shown in Fig. 1 (a). Glass beads with diameter $d = 101 \mu\text{m}$ drain from the silo into a bottom collecting chamber through an exit slot. The flow rate is set by varying the width w of the slot. A minimum width ($w = 3.25d$) was needed to observe steady flow, and the data reported here was obtained for $w = 3.5d; 4d; 5d$ and $6d$. To measure the flow away from the sidewalls, the entire system is immersed in an interstitial fluid [6] with the same refractive index ($n = 1.52$) as the glass beads. The fluid displaced in the bottom chamber is channeled through a mesh via side chambers (not shown) into the silo at the top. This arrangement was found to effectively reduce counter flow of the interstitial fluid through the exit slot.

The grains are visualized by adding a fluorescent dye to the fluid [4]. As illustrated in Fig. 1 (a), a plane inside the silo, which is less than $0.1d$ thick, is illuminated using a 50-mW laser and a cylindrical lens, and imaged through the front wall with a digital camera. Typical images for two different planes, wherein the particles appear dark against a bright background, are shown in insets to Fig. 1 (b), (c). The apparent size of the particles depends on the distance of the bead center from the laser illumination plane. A centroid algorithm is used to find sub-pixel resolution particle position with centers within $0.3d$ of the laser sheet. Imaging at 60 frames per second is sufficient to track the particles over long time periods and obtain mean velocities to within 1%.

The granular flow in the silo can be divided into two distinct regions: a convergent accelerating flow close to the exit slot and a steady plug-like flow with small shear at the walls in the region above $z = 70d$. The competition between grains exiting from the orifice results in packing density fluctuations which diffuse up through the silo as grains fall down and has been discussed previously [17]. As we are primarily interested in the fluctuation properties of the flow, we focus on the relatively simpler uniform flow region at the top.

We first examine the packing structure of the particles at various locations in the silo. The grain packing as seen in typical images corresponding to $y = 0.5d$, and $y = 5d$ in Fig. 1 (b), (c) are qualitatively different. In order to quantitatively measure the difference, we calculated the two-point spatial correlation function $g(r)$ as a function of particle separation distance r in a y plane for $y = 0.5d; 5d$, and $10d$ [see Fig. 1 (b), (c)]. While $g(r)$ corresponding to $y = 0.5d$ show stronger peaks, $g(r)$ for $y = 5d$ and $y = 10d$ are indistinguishable and the

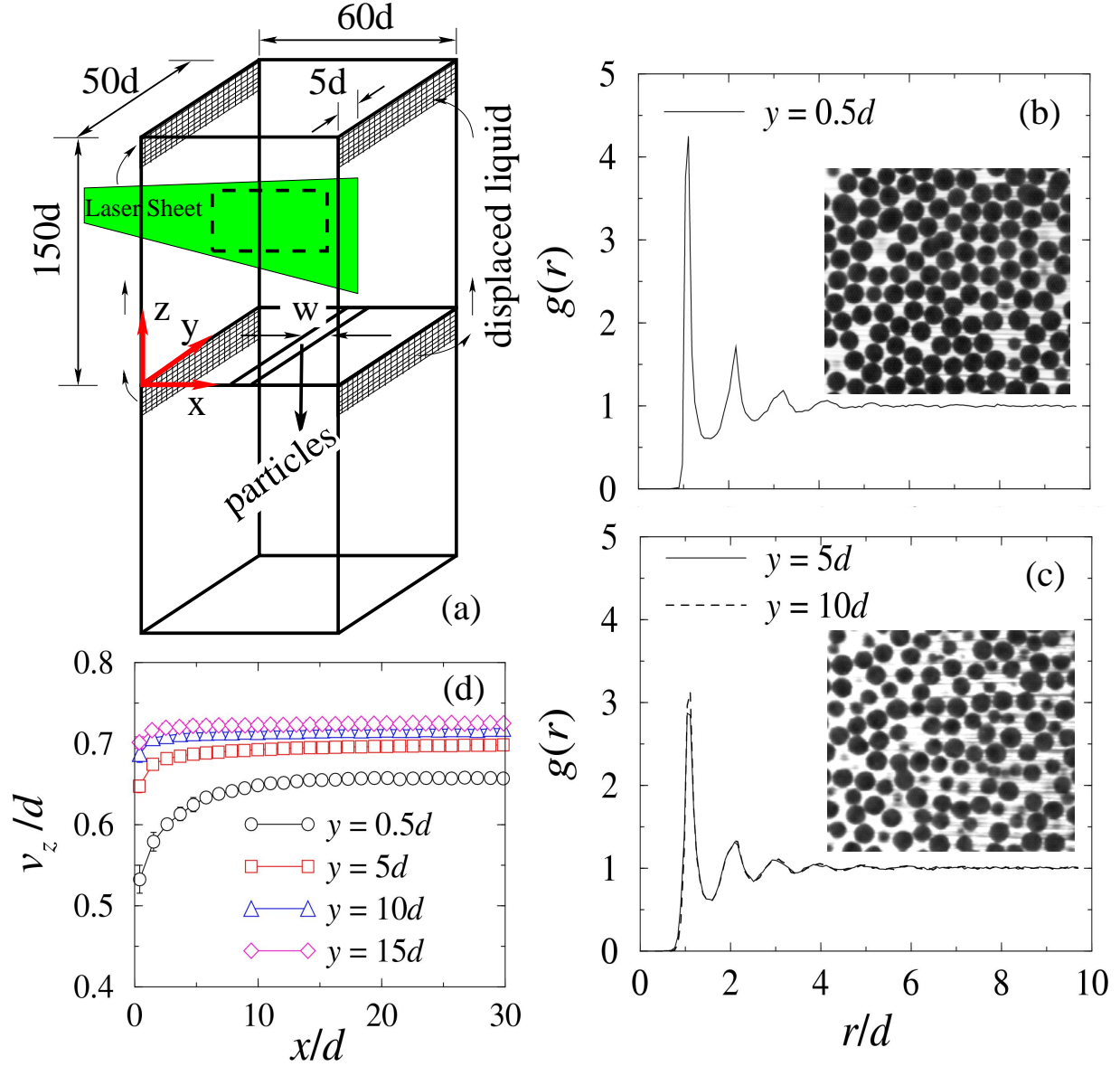


FIG. 1: (a) The schematic diagram of the silo apparatus. A laser sheet illuminates a cross section of particles in a plane at a distance y from the front surface. (b) The two-point spatial correlation function $g(r)$ of the grains located next to the front wall of the silo ($y = 0.5d$). Inset: A typical image of the grains. (c) $g(r)$ in a plane $y = 5d$ and $y = 10d$. Inset: A typical image for $y = 5d$. (d) The vertical component of the velocity v_z as a function of distance x along the horizontal axis at $y = 0.5d, 5d, 10d$ and $15d$ ($w = 4.0d$). Error bars show the deviations over 10 runs.

packing structure does not change significantly any further distance from the boundaries. The packing fraction of the beads inside the silo is measured to be 0.5965 ± 0.0123 and is observed to be independent of flow rate. Furthermore, $g(r)$ in the flowing regions is similar to that measured when the grains are at rest.

The vertical component of the velocity v_z as a function of horizontal distance is plotted in Fig. 1 (d) for grains at various distances from the front wall. Because the flow is symmetric about $x = 30d$, we show only the left half. The velocity increases with distance away from the sidewalls over a distance of about $10d$, beyond which it remains more or less constant.

In the subsequent analysis, we focus in the central nearly shear free region, of size $20d$ across and $20d$ in the flow direction, where the velocity magnitude varies within 2%. The fluctuation properties are then computed in this region for each plane y from the trajectories of individual particles. The horizontal particle displacement $\Delta x = x(t + \Delta t) - x(t)$ and the vertical particle displacement $\Delta z = z(t + \Delta t) - z(t) - V \Delta t$ in the reference frame of the flow are determined over a time interval Δt , and time averaged uniform mean flow V at the silo center ($x = 30d$). The normalized probability density functions (PDF) for Δx and Δz in the plane $y = 10d$ for $\Delta t = d/V$ are shown in Fig. 2 (a) and (b), respectively, for different flow rates. The PDFs are nearly same for the various flow rates, and are non-Gaussian similar to observations in dry granular silo flows near the side walls [1, 12]. The ratio of mean square deviations of the PDFs in the vertical to the horizontal directions is 1.33, and is similar to that in dry granular silo systems [11]. The anisotropy arises because energy is fed into the system by grains falling down under gravity and lost due to dissipative collisions with neighbors in all directions. Non-Gaussian PDFs have been observed in colloidal glasses [6] as well and are attributed to cage breaking and depends on the time interval Δt used to calculate the displacements.

The deviation of the PDFs from a Gaussian distribution is determined using the normalized kurtosis, defined as $\kappa = \langle \Delta^4 \rangle / 3 \langle \Delta^2 \rangle^2 - 1$, where $\Delta = \Delta x; \Delta z$. The kurtosis for Δx and Δz as a function of normalized Δt is shown in Fig. 2 (c) and (d), respectively. In all cases, kurtosis decreases inversely with time to zero indicating an approach to diffusive motion as grains undergo several rearrangements.

To characterize the fluctuations further, we plot the mean square horizontal $\langle \Delta x^2 \rangle$ and vertical $\langle \Delta z^2 \rangle$ displacements in the flow frame of reference versus distance traveled with the flow (and thus time) in Fig. 2 (e,f). Above the noise floor, we find that $\langle \Delta^2 \rangle$ increase

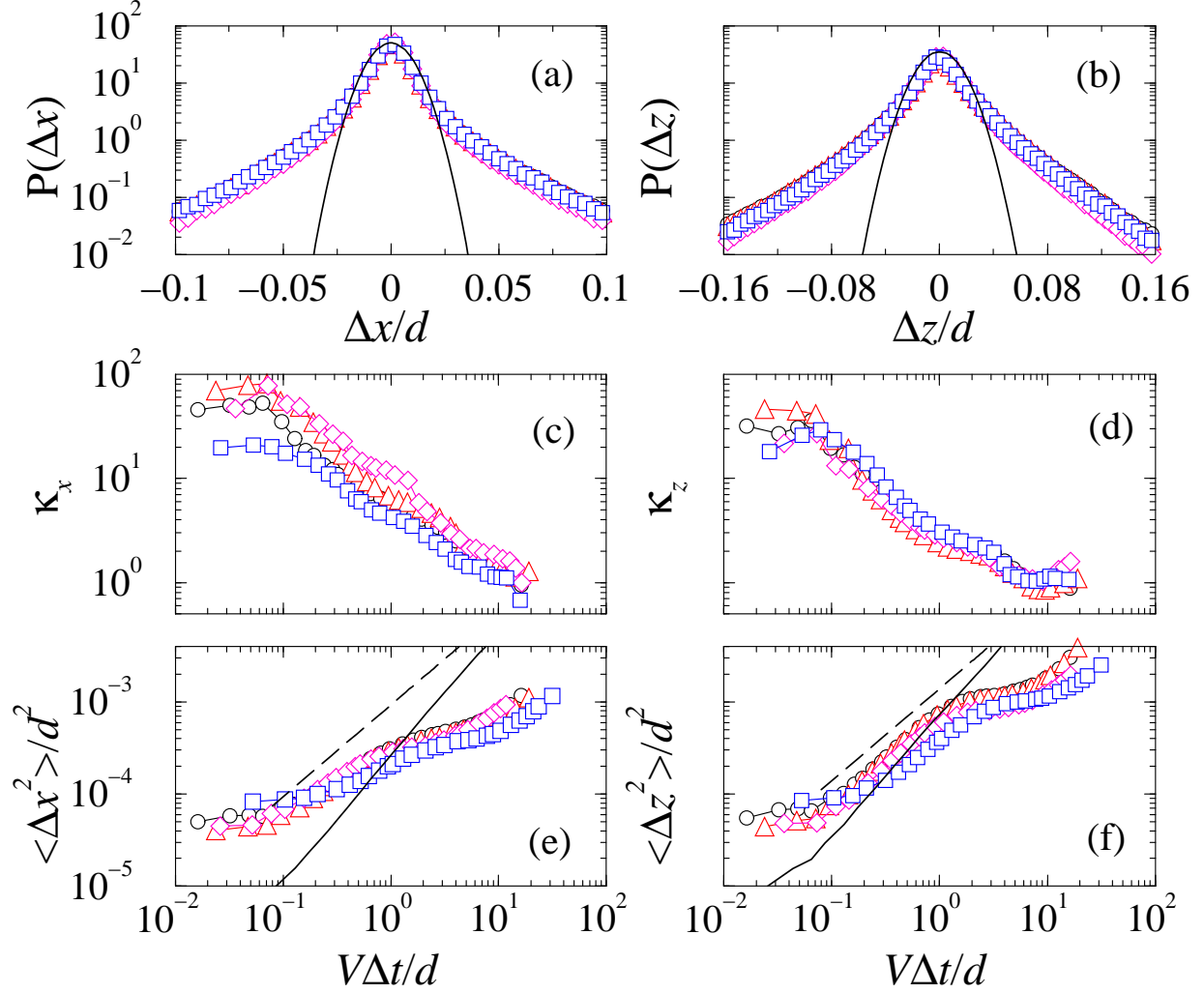


FIG. 2: (a, b) Probability distribution function (PDF) of particle displacements, x and z , measured over a time interval $t = 1d/V$ in the plane $y = 10d$. $\phi = 0.5d=s$, $\phi = 0.7d=s$, $\phi = 1.1d=s$, $\phi = 1.6d=s$, Gaussian distribution (solid line). (c,d) The kurtosis of the x and z PDFs versus the mean distance traveled. (e,f) The horizontal and vertical mean square displacement versus mean distance traveled by the grains. Dashed line of slope 1 corresponds to a purely diffusive flow. Solid line correspond to $y = 0.5d$ and $V = 0.7d=s$.

approximately linearly, shows an inflection point, and then curves up to approach a linear increase corresponding to diffusive motion. $\langle x^2 \rangle$ is somewhat lower in comparison with $\langle z^2 \rangle$ just as for the PDFs. The inflection point and linear to linear behavior seen here is qualitatively similar to observations in elastic hard sphere suspensions for densities near the glass transition [6, 7]. There the inflection point is associated with a slow coherent cage

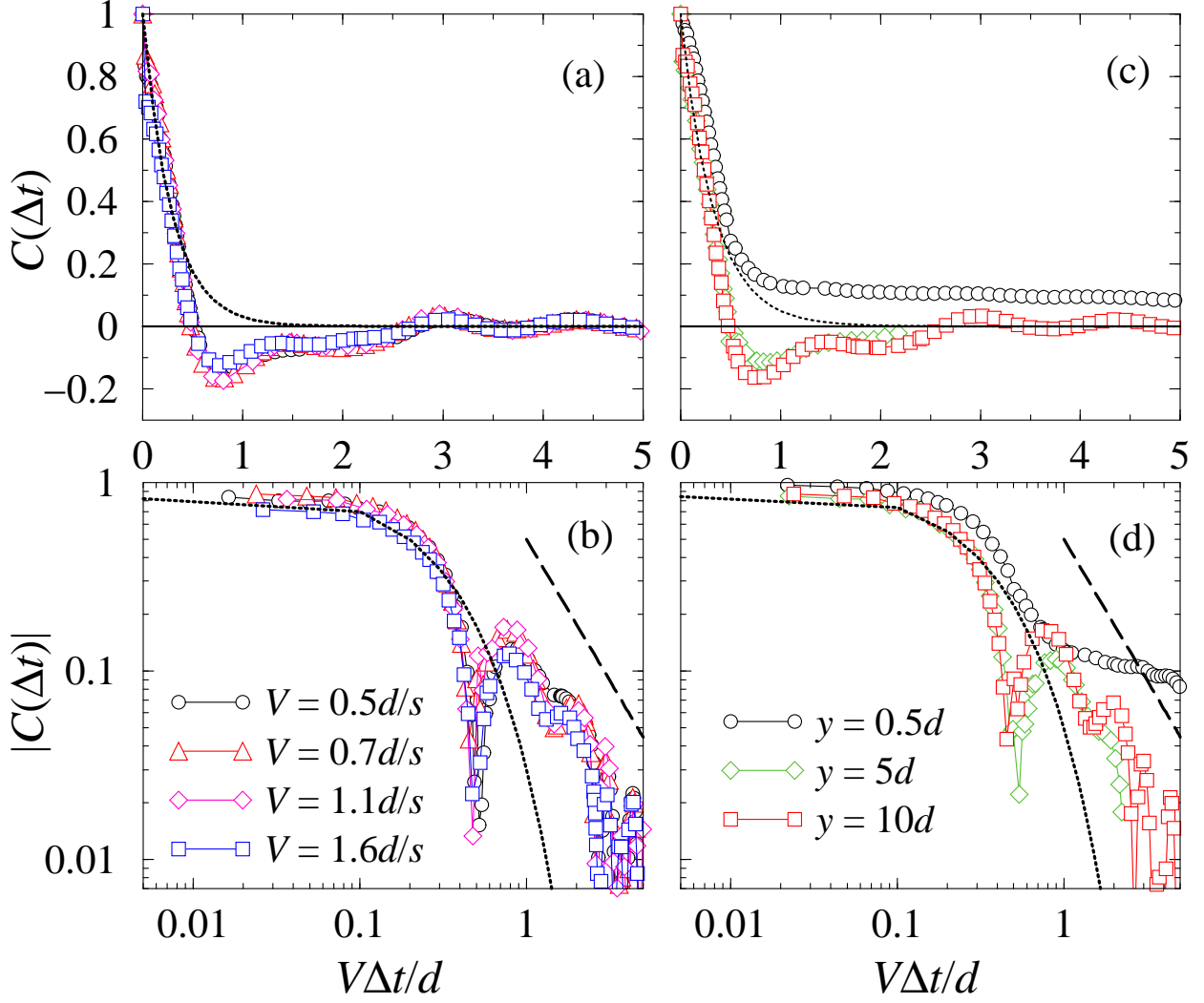


FIG. 3: The velocity auto-correlation function $C(t)$. (a,b) Effect of flow rate. Data for the plane $y = 10d$, and (c,d) Effect of end walls. Data for mean flow velocity $V = 0.7d/s$. Velocities calculated using a time interval $\Delta t = 0.5d/V$. Dotted line represents an exponential decay while dashed line represents long time power law decay ($t^{-3/2}$).

breaking motion that takes longer time to develop and diverges as the volume fraction is increased. The mean square displacements at the boundaries [solid lines in Fig. 2 (e),(f)] show a very different behavior (slope -1.4). But it is noteworthy that it is in agreement with the experimental results measured for dry granular flows at the boundaries [1, 12].

To gain further information on the cooperative nature of the fluctuations, we next turn to velocity correlations and examine the velocity auto-correlation function (VAF). For grains

in a given y plane, the instantaneous fluctuating velocity components (u_x, u_z) at any time instant are obtained by subtracting the mean flow velocity at that instant from the individual velocities of the grain. The VAF is, then, calculated from the measured velocities using the definition $C(t) = \langle u_x(t)u_x(t+t) + u_z(t)u_z(t+t) \rangle$, where the angled brackets represents the averaging over all times t of flow. The VAFs for $y = 10d$ is shown using linear scale in Fig. 3(a) and double-log scale in Fig. 3(b). The profiles are distinctly different from an exponential decay (dotted line) displayed by a Brownian particle obeying the Langevin equation. In particular, it may be noted that VAF becomes negative over a time scale comparable to the time taken for the grains to flow about a grain diameter, irrespective of the flow rate. Then, the VAF oscillates and decays to zero over long times. The magnitude of the negative correlation and the overall shape of the decay is very similar to that observed first by Rahman [2] in simulations of liquid Argon, and more recently in the molecular dynamics simulations of meta-stable liquids at high volume fractions by Williams, et al [18].

The negative correlations and slow decay in dense liquids are said to arise due to back-scatter of the tagged particles and reversal of velocity into a comparatively narrow range of angles, and development of a back flow [1]. Because many particles are involved in this process, a hydrodynamic model was developed to describe the correlations [3, 4]. The model gives a $3/2$ scaling for the decay of the correlations due to the diffusion of momentum of the tagged particle. This scaling is denoted by the dashed line in Fig. 3(b,d). Although the data is consistent with $3/2$ scaling, our observation time window is rather limited.

The data corresponding to grains next to the front wall and at various depths y is shown in Fig. 3(c,d). The behavior is qualitatively different at the walls and negative VAFs are not observed. It is possible that differences can arise for the following reasons. The particles in the bulk can move in all three directions, so the fluctuations diffuse faster than those at the walls which limit grain fluctuation in that direction. Further, as can be seen from Fig. 1(b,c), the grains near the wall appear more structured which may also lead to differences. The boundaries also induce shear and Kumaran [19] has recently argued that VAFs can decay faster in sheared granular flow than for fluids in equilibrium. However, these effects appear to be not so strong when comparing the results at the boundaries.

The implied velocity fields can be tested statistically using the spatial velocity correlation function defined as $C(r) = \langle u_x(r_0)u_x(r_0 + r) + u_z(r_0)u_z(r_0 + r) \rangle$. The angled brackets represents the averaging over all particle centered at r_0 and over all the measurement time

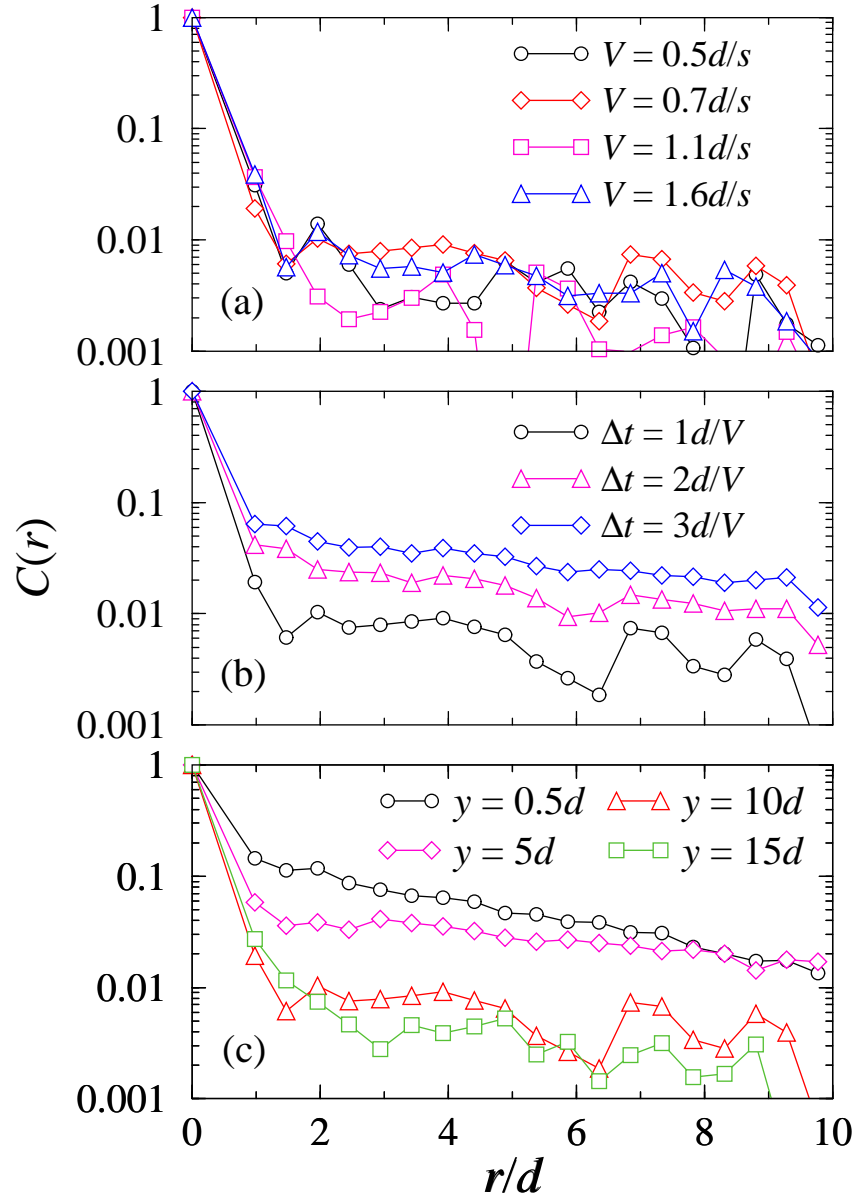


FIG. 4: Spatial velocity correlation $C(r)$ versus the interparticle distance $r=d$. (a) Effect of flow rate. ($t = d/V$) (b) Effect of the averaging time interval. ($y = 10d$ and $V = 0.7d/s$) (c) Effect of the side walls. ($t = d/V$ and $V = 0.7d/s$).

window for particles separated by a distance r . The measured $C(r)$ for various flow rates is shown in Fig. 4(a) where the velocity has been calculated over a time interval $t = d/v_z$ corresponding to the minimum in $C(t)$. (Separate correlations for the x and z components were found to be similar, and therefore the averaging over r is reported here to consolidate

the graphs.) Only weak spatial velocity correlations close to the noise floor may be noted over this time scale. $C(r)$ increases modestly if the velocity is calculated over a longer time interval corresponding to the slow decay observed in $C(t)$ [see Fig. 4(b)]. Therefore while a signal of cooperative flow is observed, it appears to be rather weak perhaps because the cooperative motion is spread over a large number of particles.

To compare the spatial correlations observed in the bulk with those at the boundaries, $C(r)$ is plotted for various planes from the front wall (see Fig. 4(c)). It can be noted that significantly greater spatial correlations are observed near the boundaries. The strength of correlations is in fact similar to that observed in dry granular flows where observations have been made only next to the side walls and where shear is present [10, 12]. Thus the correlations as measured by mean square deviations, $C(t)$, and $C(r)$ are consistently different in the shear free bulk flow regions and at the boundaries. Further work is required to distinguish between the contribution due to the screening and ordering induced by the boundaries, and the contribution due to shear.

Finally, we discuss the effect of the interstitial fluid on the reported fluctuation properties of the grains. In principle, viscous forces due to the interstitial fluid exist between particles which can affect their fluctuations. These forces are directly proportional to the relative velocity and thus rate dependent. However, as the PDFs, $\langle x^2 \rangle$, $\langle z^2 \rangle$, and $C(t)$ coincide when plotted over distance traveled in the flow, irrespective of flow rate, we conclude that any rate dependent forces introduced by the interstitial fluid has insignificant effect on the fluctuation properties discussed here. This argument, along with our observations that the fluctuation properties near the side walls are consistent with that of dry granular systems reported previously, indicates that our results are applicable to dry granular flows in the bulk as well.

In conclusion, the correlations in fluctuations observed for grains undergoing uniform flow are remarkably similar to that exhibited by an elastic hard-sphere liquid. In hydrodynamic models of elastic hard-spheres, the Enskog equation is used to calculate transport coefficients, which includes the finite size of the particles but ignores the velocity correlations built up by successive collisions [1]. Our observations seem to indicate that the dissipative nature of the grain-grain interaction do not significantly change the corresponding correlations in granular systems, and suggests that a similar approach may be fruitful for dense granular flows.

We thank J. Norton for his help with the apparatus. This work was supported by the National Science Foundation under grant number CTS-0334587, and the donors of the Petroleum Research Fund.

-
- [1] J. P. Hansen and I. R. McDonald, *Theory of Simple Liquids* (Academic Press, New York, 1991).
 - [2] A. Rahman, *Phys. Rev.* **136**, A 405 (1964).
 - [3] B. J. Alder and T. E. Wainwright, *Phys. Rev. A* **1**, 18 (1970).
 - [4] R. Zwanzig and M. Bixon, *Phys. Rev. A* **2**, 2005 (1970).
 - [5] Y. Pomeau and P. Resibois, *Phys. Rep.* **19**, 63 (1975).
 - [6] E. R. Weeks and D. A. Weitz, *Phys. Rev. Lett.* **89**, 095704 (2002).
 - [7] W. van Megen, *J. Phys.: Condens. Matter* **14**, 7699 (2002).
 - [8] J. W. Dufty and J. J. Brey, *Phys. Rev. E* **68**, 030302(R) (2003).
 - [9] N. Menon and D. J. Durian, *Science* **275**, 1920 (1997).
 - [10] D. M. Muth, *Phys. Rev. E* **67**, 011304 (2003).
 - [11] J. Choi, A. Kudrolli, R. R. Rosales, and M. Z. Bazant, *Phys. Rev. Lett.* **92**, 174301 (2004).
 - [12] S. Moka and P. R. Nott, *Phys. Rev. Lett.* **95**, 068003 (2005).
 - [13] O. Poulliquen, *Phys. Rev. Lett.* **93**, 248001 (2004).
 - [14] S. Siavoshi, A. V. Orpe, and A. Kudrolli, *Phys. Rev. E* **73**, 010301(R) (2006).
 - [15] J.-C. Tsai, G. A. Voth, and J. P. Gollub, *Phys. Rev. Lett.* **91**, 064301 (2003).
 - [16] The liquids were obtained from Cargille Laboratories, and have a density of 1100 kg m^{-3} and viscosity of $2 \times 10^{-5} \text{ m}^2 \text{ s}^{-1}$.
 - [17] J. Mullins, *J. Appl. Phys.* **43**, 665 (1972); M. Z. Bazant, *Mech. Mater.* **38**, 717 (2006).
 - [18] S. R. Williams, G. Bryant, I. K. Snook, and W. van Megen, *Phys. Rev. Lett.* **96**, 087801 (2006).
 - [19] V. Kumaran, *Phys. Rev. Lett.* **96**, 258002 (2006).